REVIEW OF SOME CALCULATIONS OF ENERGY TRANSPORT IN A GARRETT-MUNK OCEAN

Neil Pomphrey
Center for the Studies of Nonlinear Dynamics
of La Jolla Institute
P.O. Box 1434
La Jolla, CA 92038

ABSTRACT

A review of current understanding of energy redistribution processes within the ocean internal wave field will be given. Relaxation rates for "test waves" in a Garrett-Munk model ocean have mainly been calculated using Hasselmann transport theory or related methods. Computations show that GM76 is approximately a steady state spectrum for 3-wave interactions except for frequencies near the inertial frequency and at the lowest vertical mode-numbers. The lack of variation of the internal wave coupling coefficients allows discussion of results in terms of McComas and Bretherton's three limiting mechanisms; Induced Diffusion, Elastic Scattering and Parametric Subharmonic Instability. In the high vertical modenumber regime Induced Diffusion provides the most significant contribution. Transfer rates are high here and there has been concern for the validity of the Hasselmann theory. However, recent calculations by Meiss and Watson which relate Induced Diffusion to the Taylor Goldstein equation yield relaxation rates which are valid over a much extended domain.

INTRODUCTION

Within the last five years considerable progress has been made in understanding the role of wave-wave interactions in redistributing energy and in determining the spectral shape of oceanic internal waves. The calculations which have led to this understanding have mostly been based on the notion that the internal wavefield is weakly turbulent and representable as a statistical ensemble of weakly coupled wave modes. In this case a transport theory due to Hasselmann is valid which provides an evolution equation for action density in wavenumber space ensemble averaged over realizations of the chosen wavefield.

The earliest detailed calculations which used the Garrett-Munk spectrum to represent the chosen wavefield were performed by Olbers and by McComas and Bretherton. The latter work was particularly important for its identification of the three limiting triad mechanisms named Induced Diffusion, Elastic Scattering and Parametric Subharmonic Instability. In terms of these mechanisms the computed energy transfer rates were readily understood, and a physically appealing "scenario for the genesis and maintenance of the universal (internal wave) spectrum" was provided.

An inconsistency was immediately apparent between computed results and assumptions made by the underlying theory: At the intermediate and high

0094-243X/81/760113-16$1.50

internal wave frequencies where Induced Diffusion is the dominant transfer mechanism, energy transfer times are shorter than a wave period. A different theory is required here.

Meiss and Watson have recently exploited a relationship between Induced Diffusion and a time-dependent form of the Taylor-Goldstein equation to derive transfer rates for Induced Diffusion which avoid any weak interaction assumption. These (corrected) rates are considerably lower than those previously predicted; however, no substantial modification of McComas and Bretherton's transfer picture is required.

WEAK INTERACTION THEORY

The wide success of the Garrett-Munk (GM) models[1,2] which use linearized wavefunctions and wave dispersion to relate measurements has suggested that a sensible first approximation should treat interactions between internal waves as weakly nonlinear. This allows the use of a number of tractable methods for studying energy transport within the internal wavefield. Most popular among these is the transport theory due to Hasselmann[3], which leads to an equation for the evolution of action density in wavenumber space.

As the starting point we shall take the set of (Fourier) mode equations for (complex) amplitudes of fluid displacement. These are derived from the inviscid fluid equations with little difficulty and take the form[4]

$$\frac{d}{dt} a_{\underline{k}} + i\omega_{\underline{k}} a_{\underline{k}} = \sum_{\underline{\ell},\underline{m}} \left[\delta_{\underline{k}-\underline{\ell}-\underline{m}} \; G^{\underline{k}}_{\underline{\ell}\,\underline{m}} \, a_{\underline{\ell}} a_{\underline{m}} + \delta_{\underline{k}+\underline{\ell}-\underline{m}} \; G^{\underline{k}\ell}_{\underline{m}} \; a^{*}_{\underline{\ell}} \, a_{\underline{m}} + \delta_{\underline{k}+\underline{\ell}+\underline{m}} \, G^{\underline{k}\ell\underline{m}} \; a^{*}_{\underline{\ell}} \; a^{*}_{\underline{m}} \right] . \tag{1}$$

In the linear approximation when the right hand side (RHS) is zero, the $a_{\underline{k}}$ represent amplitudes of travelling plane waves having wavenumber $\underline{k}$ and frequency $\omega_{\underline{k}}$. Wave triad terms appear on the RHS and arise from quadratically nonlinear terms in the fluid equations. For an ocean model with buoyancy (Vaisala) frequency N(z) = constant, independent of depth z, an Eulerian derivation[5,6] gives equation (1) exactly whereas a Lagrangian derivation[7-10] yields (in more complicated fashion) modified coupling coefficients

$$G^{\underline{k}}_{\underline{\ell}\,\underline{m}} \longrightarrow G^{\underline{k}}_{\underline{\ell}\,\underline{m}} + (\omega_{\underline{k}} - \omega_{\underline{\ell}} - \omega_{\underline{m}}) \Delta^{\underline{k}}_{\underline{\ell}\,\underline{m}} \quad , \text{etc.} \tag{2}$$

as well as wave quartets and higher order interactions. We note, however, that to lowest order of nonlinearity the resonant (physical) energy exchange between modes is independent of representation.

A complete description of the wavefield requires zero (linear) frequency Horizontal Eddy Modes[11] as well as those with frequencies between the coriolis and buoyancy limits. The coupling between these two types of mode vanishes on resonance and therefore gives no contribution to internal wave energy transport at lowest order (on the other hand momentum transport is affected by Eddy scattering). We will see later, however, that a satisfactory description of

energy transport by the important Induced Diffusion mechanism requires consideration of off-resonant triads and the influence of the Eddy modes here should be investigated.

There are several recipes for proceeding from the evolution equations for mode amplitude $a_{\underline{k}}$ to closed evolution equations for average wave action $\langle J_{\underline{k}} \rangle \equiv \langle |a_{\underline{k}}|^2 \rangle$[12-14]. For all of these it is sufficient to consider a subdivision of the entire wavefield, the test wave system. Here the test wave is a labelled wave (given subscript $\underline{k}$, say) whose properties are to be monitored. Many (∞) pairs of background waves interact with the test wave and couple with one another only through the test wave as intermediary. There is no direct coupling between ambient members of different triads[15].

An essential ingredient of all recipes is the assumption:

(A1) There exists a time scale separation between fast linear oscillation ($\tau_{\text{linear}} \sim \frac{1}{\omega_{\underline{k}}}$) and slow nonlinear transfer ($\tau_{\text{nonlinear}} \sim \frac{1}{\nu_{\underline{k}}}$):

$$\nu_{\underline{k}} \ll \omega_{\underline{k}}. \tag{3}$$

This allows the use of multiple time scale perturbation theory. On the slow time scale transfer results to lowest order from secular growth of the action on account of wave triads that satisfy a resonance matching condition between linear frequencies[16]

$$\omega_{\underline{k}} \pm \omega_{\underline{\ell}} - \omega_{\underline{m}} = 0 \tag{4}$$

Finally, to evaluate the transfer rate $\nu_{\underline{k}}$ in terms of known quantities requires a closure assumption in the form of:

(A2) The Random Phase Approximation[17-18]. This assumes that wave phases decorrelate rapidly compared with the transfer time so that (operationally) fourth and higher order cumulants can be discarded, and fourth moments expressed as products of second moments (actions). Although it is clear that nonlinear interactions between the test wave system and complementary waves must lead to some phase randomizing, the extent to which this happens is not controlled in the calculation so this last assumption requires an act of faith.

The resulting transport equation is the familiar wave analogue of the particle Boltzmann equation

$$\frac{d}{dt}\langle J_{\underline{k}} \rangle = \sum_{+,-} \int d\underline{\ell}\, d\underline{m}\, \delta(\omega_{\underline{k}} \pm \omega_{\underline{\ell}} - \omega_{\underline{m}})\, \delta(\underline{k} \pm \underline{\ell} - \underline{m})$$
$$\times |\Gamma^{\pm}|^2 \left\{ \langle J_{\underline{\ell}} \rangle \langle J_{\underline{m}} \rangle - J_{\underline{k}} \left(\langle J_{\underline{\ell}} \rangle \pm \langle J_{\underline{m}} \rangle \right) \right\} . \tag{5}$$

The source function on the RHS comprises an integral over the kinematic region, represented by the frequency and momentum delta function, of a product of two factors: $|\Gamma^{\pm}|^2$ is a geometric factor formed out of simple combinations of the G-coupling coefficients of the dynamical equations[19]. The second factor contains the specification of the ambient spectrum and has nothing to do with the dynamics. For the calculations to be described shortly each angle bracket represents one of the GM model action spectra.

It is useful to rewrite equation (5) in schematic form:

$$\frac{d}{dt}\langle J_{\underline{k}}\rangle = I(\underline{k}) - 2\nu_p \langle J_{\underline{k}}\rangle \quad . \tag{6}$$

The quantity $I(\underline{k})$ arises from the product of the $\underline{\ell}$- and $\underline{m}$-wave actions. It represents excitation of the test wave by coalescent scattering of background waves, and feeds action into wavenumbers near $\underline{k}$[20]. The second term (which defines the coefficient ν_p) has an identity that is quite independent of the transport equation. It can be derived using Langevin methods[19] and does not require a random phase approximation. ν_p is the autocorrelation decay rate of an arbitrary initial wave amplitude, and is of fundamental importance for understanding energy transport processes. Finally, a Boltzmann rate can be defined as

$$2\nu_B(\underline{k}) = (I - 2\nu_p \langle J_{\underline{k}}\rangle)/\langle J_{\underline{k}}\rangle \quad , \tag{7}$$

which gives the net rate of action flow through $\underline{k}$. If the Boltzmann rate is small in some region of $\underline{k}$-values this indicates that the ambient spectrum may be a close representation of a steady state there†. If, in addition, the relaxation rate ν_p is large then any ripple added to the spectrum will be quickly smoothed by the wave interactions and a degree of universality will be apparent.

COMPUTED TRANSFER RATES USING W.I.T.

The early detailed calculations[21] which used GM spectra as input were performed by Olbers[8] and by McComas and Bretherton[9]. They used an exponential buoyancy profile

$$N(z) = N_o e^{z/B} \tag{8}$$

and a WKB approximation to provide a dispersion relation and to evaluate the coupling coefficients, but assumed a constant value of N throughout a box within which three-dimensional wave propagation is confined. Later calculations by Watson et. al.[10,19] used an exponential profile throughout the box, and discrete modes for the vertical direction. The two approaches are essentially equivalent except at the lowest modenumbers, and to relate the calculations we can use the WKB relation

$$k_z B \simeq j\pi \frac{N(z)}{N_o} \tag{9}$$

which matches (integer) modenumber j with local vertical wavenumber k_z.

In broad terms the results of these calculations show a systematic transfer of wave energy (action x frequency) into near-inertial frequencies and

†It is important to distinguish between steady state and equilibrium.

towards smaller vertical wavelengths. Much of the spectrum, however, appears to be near steady state. For a measure of this it is useful to consider the ratio (R) of net Boltzmann rate to test wave excitation rate[19]. This measure of action throughput of a region divided by action input is plotted as a function of linear wave frequency (in units of coriolis frequency f) in Figure 1. Each curve

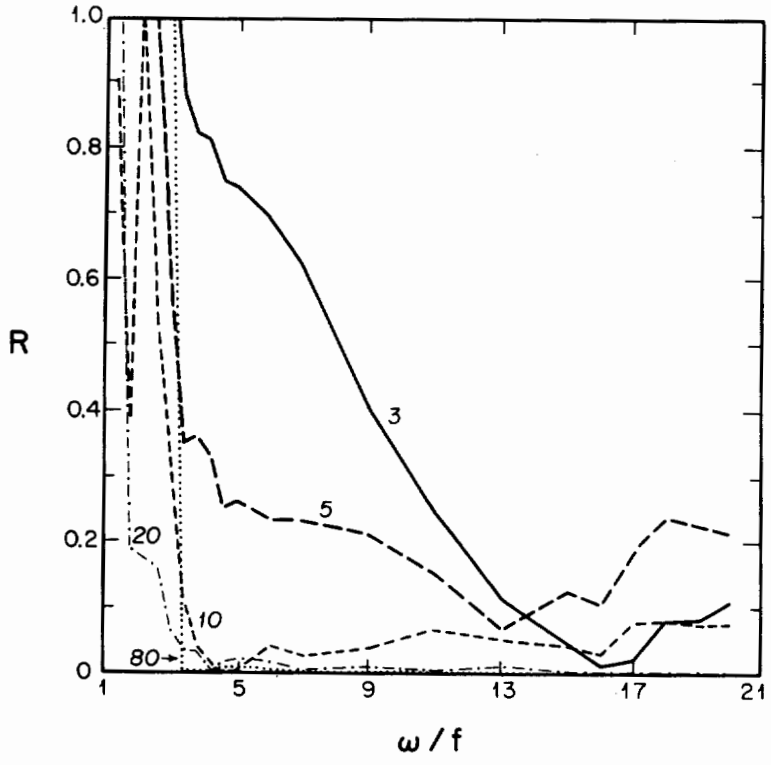

Figure 1. Numerical evaluation of the ratio (R) of net Boltzmann rate to test wave excitation rate. Curves are labelled by a value of mode-number.

is labelled by a value of modenumber. For modenumbers $j \gtrsim 10$ and frequencies $\omega \gtrsim 3f$ the ratio is seen to be small. In particular, for $j = 10$, R is less than five percent in this region. For high modenumbers (> 100), R is found to be fractions of one percent indicating a domain close to steady state. To obtain a picture of energy transfer across the wavefield we can arbitrarily define a 'steady state' to be one in which $R < 10\%$. Figure 2 results from using the GM 76 model spectrum. Here the steady region is unshaded whereas the shaded (nonsteady) regions show the sign of the Boltzmann rate to indicate whether energy is growing (+ values) or being depleted (- values). Specifically then, energy flow is seen to be from low modenumbers and most frequencies into intermediate and high modenumbers at low frequencies. Both Olbers and

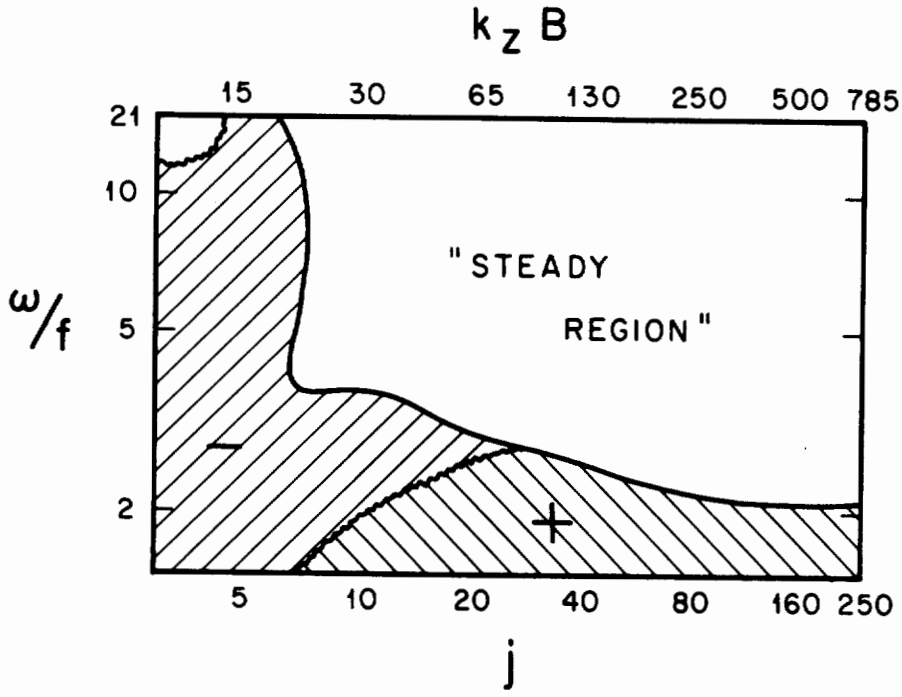

Figure 2. Evergy growth (+) and energy decay (-) regions using the GM76 model spectrum. The "steady" region is where R < 10%.

McComas and Bretherton estimate the energy transfer rate across GM 75 to be 3×10^{-3} Wm^{-2} which gives an energy turnover time of approximately 10 days. For GM 76 and using discrete modes, Pomphrey, Meiss and Watson[19] estimate a somewhat lower value of 6.4×10^{-4} Wm^{-2}. Both estimates can easily be faulted, nevertheless they suggest a figure near 1×10^{-3} Wm^{-2} in reasonable agreement with Leaman's observational data[22] of downward energy flux beneath the thermocline.

Although the source function which determines the results couples triads from a continuum of scales, McComas and Bretherton greatly increased our understanding of the underlying dynamics by identifying three simple triad classes which appear to dominate the transfer. This simplification is possible, in large part, because of the small variation of the dynamical factor in the source function compared with the spectral factor. To illustrate this we show contours of $|\Gamma^{\pm}|^2$ using a "box representation" (Figure 3):
If for any three waves with horizontal wavenumbers $\underline{k}$, $\underline{\ell}$ and $\underline{m}$ we plot $|\underline{m}|$ versus $|\underline{\ell}|$ for a given value of test wavenumber $\underline{k}$, triads which satisfy the momentum condition

$$\underline{k} \pm \underline{\ell} - \underline{m} = 0 \qquad (10a)$$

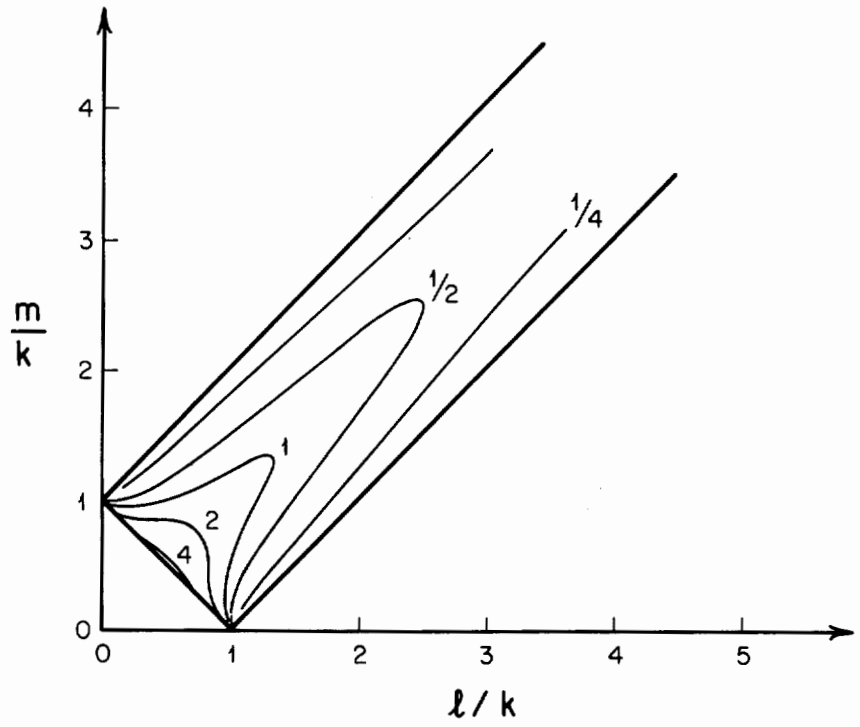

Figure 3. Contours of the dynamical factor $|\Gamma^{+}|^2$ of the source function in equation (5) using a "box representation" to define the kinematically allowed region.

must lie on or within an open rectangle whose corners intersect the axes at $|\underline{m}| = |\underline{k}|$ and $|\underline{\ell}| = |\underline{k}|$. Triads which correspond to points lying on a box boundary have colinear wavevectors. The frequency conditions

$$\omega_{\underline{k}} \pm \omega_{\underline{\ell}} - \omega_{\underline{m}} = 0 \tag{10b}$$

further restrict a given triad to lie on a curve within the kinematic box. In the absence of a coriolis frequency these curves are straight lines whose slope (use the dispersion relation for internal waves) depends only on the relative magnitudes of vertical wavenumber restricted by

$$k_z \pm \ell_z - m_z = 0 \quad . \tag{10c}$$

When f is included, lines are bent into curves with the curvature small except in the vicinity of the box corners.

Figure 3 shows a plot of $|\Gamma^{+}|^2$ obtained for f = 0. There is seen to be little variation of this coefficient throughout the kinematic box. On the other hand the strong wavenumber dependence of GM spectra allows a variation of the spectral factor which spans several decades. It follows that not only does the spectral factor of the source function determine the signature of transfer, but it also determines much of the relative strength also, with transfer strongest when there exists an action imbalance between triad members.

Two of the triad classes identified by McComas and Bretherton have members with widely separate frequencies (Figure 4): Induced Diffusion (I.D.) consists of two nearly identical high frequency waves (one of them is the test-wave) which interact with a near inertial wave of much smaller wavenumber. The name Induced Diffusion arises because for an arbitrary spectrum the low frequency waves can be shown to act as a catalyst for diffusion of wave action. For GM spectra diffusion is strongest in the vertical z-direction. Spectra for which there exists equipartition of action among vertical modes are in diffusive steady state with respect to this mechanism. GM76 has such an equipartitioned form at high modenumber. A second mechanism is named Elastic Scattering (E.S.). This differs from I.D. only by description of wave properties in the z-direction: Two waves with nearly equal frequency and wavenumber magnitude, but opposite vertical propagation directions, interact with a wave of much lower frequency with double the vertical wavenumber. The test wave is again one of the high frequency waves. If initially the upgoing wave has less/more energy than the downgoing wave, the two energies will approach the same value asymptotically with relaxation rate $4\,\nu_p$.

Finally, the Parametric Subharmonic Instability (P.S.I.) mechanism describes a low vertical wavenumber test wave which decays into two high vertical wavenumber waves with approximately one-half the frequency. This eventually pushes energy into the inertial band at high vertical wavenumber (recall Figure 2 which shows growth here).

The importance of these mechanisms in shaping the observed spectrum can be assessed by evaluating their relaxation rates. McComas computed numerically the initial relaxation of an appropriate bump or spike perturbation added to a GM background. Alternatively, the appropriate limits of the dynamical coupling coefficients corresponding to the three triad classes may be taken, and the summations and integrations of the source function performed explicitly to obtain analytical estimates.

Typical results are shown in Figure 5: Relaxation rate ν_p is plotted as a function of linear frequency. Each curve is labelled by a value of modenumber. At low frequencies ($\omega \lesssim 3f$) only the P.S.I. mechanism is valid. At higher frequencies the I.D. and E.S. contributions are shown. (P.S.I. remains valid but its contribution is minor and not shown.) I.D. is dominant, and in fact does a remarkable job of reproducing the full numerical evaluation of the source function. The unlabelled dashed curve that runs across the figure represents equality between relaxation rate and linear frequency. Even at moderately low modenumbers a problem is clearly evident: The linear frequency curve disects the I.D. contributions. Above and near this curve, relaxation rates are too rapid to justify the time scale separation used to derive the transport equation[26].

To summarize the transport results obtained using weak interaction theory we use Figure 6 which contains a sample of results obtained from a full evaluation of the source function in equation (5). The low frequency domain $\omega < 3f$ is dominated by the P.S.I. mechanism. Nonlinear relaxation rates are low enough that we can have some confidence that the resonant weak interaction

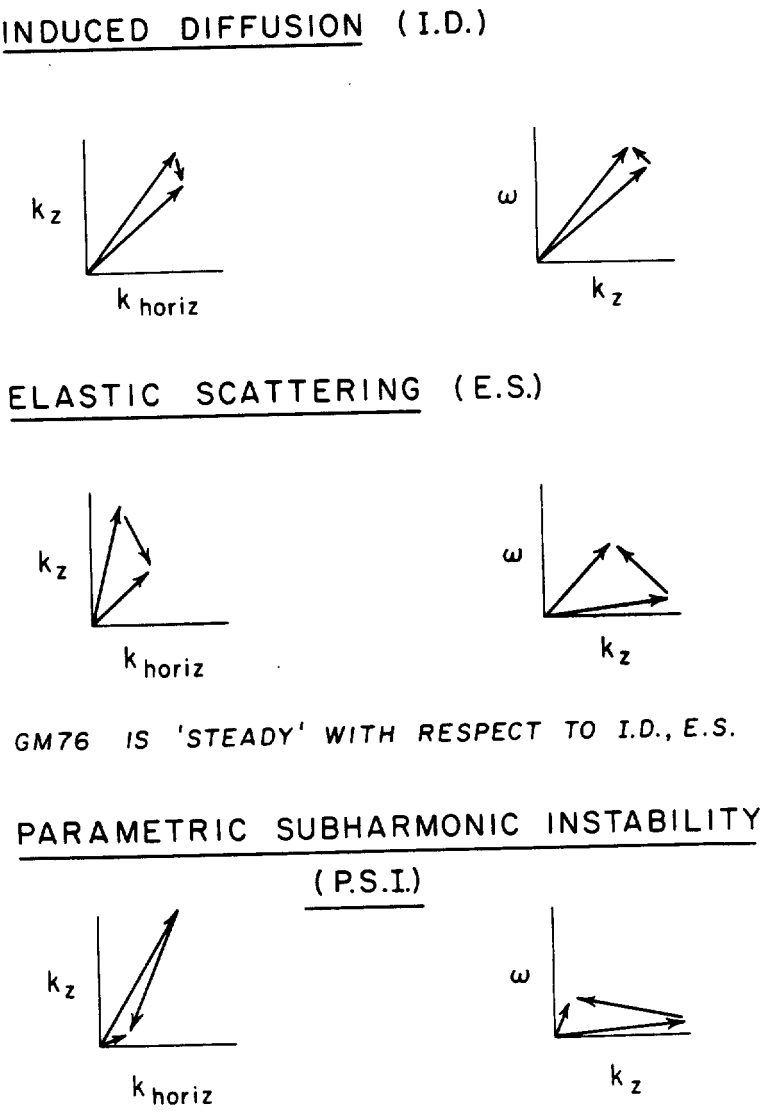

Figure 4. McComas and Bretherton's limiting triad interaction mechanisms. Their identification allows a simplified description of energy transfer within a Garrett-Munk spectrum.

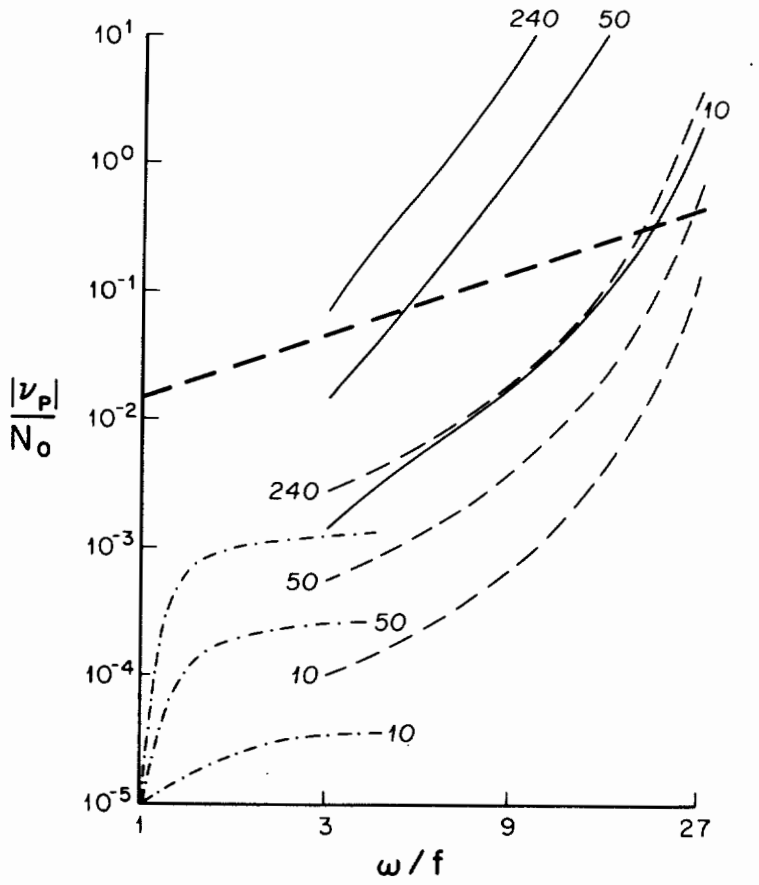

Figure 5. Analytic estimates of the relaxation rates ν_p of a spike perturbation added to a GM76 background. _____ I.D.; _ _ _ E.S.; _ · _ · _ P.S.I. The solid dashed line corresponds to $\nu_p = \omega$.

theory which led to the results may be valid. At least we can say there is no obvious inconsistency with assumptions made by the theory. For higher frequencies and vertical modenumbers $j \lesssim 10$ an assortment of triads (A.T.) gives rise to transfer and the rates are again low enough to expect the theory is valid. In a separate contribution to these Proceedings, Watson has demonstrated that the E.S. mechanism is also adequately described by weak resonant transport theory. We are left with the domain $j \gtrsim 10$ and $\omega \gtrsim 5f$ and here the story is different: the rates are dominated by I.D. and these are too high to have faith in the theory.

CORRECTED DESCRIPTION OF INDUCED DIFFUSION

The physical description of I.D. as the interaction between small scale, high frequency internal waves and a much larger scale, low frequency (near horizontal) flow suggests a relationship with the Taylor-Goldstein equation which is used to discuss the stability of stratified shear flows. Meiss and Watson[27] have recently exploited this relationship to derive relaxation rates for

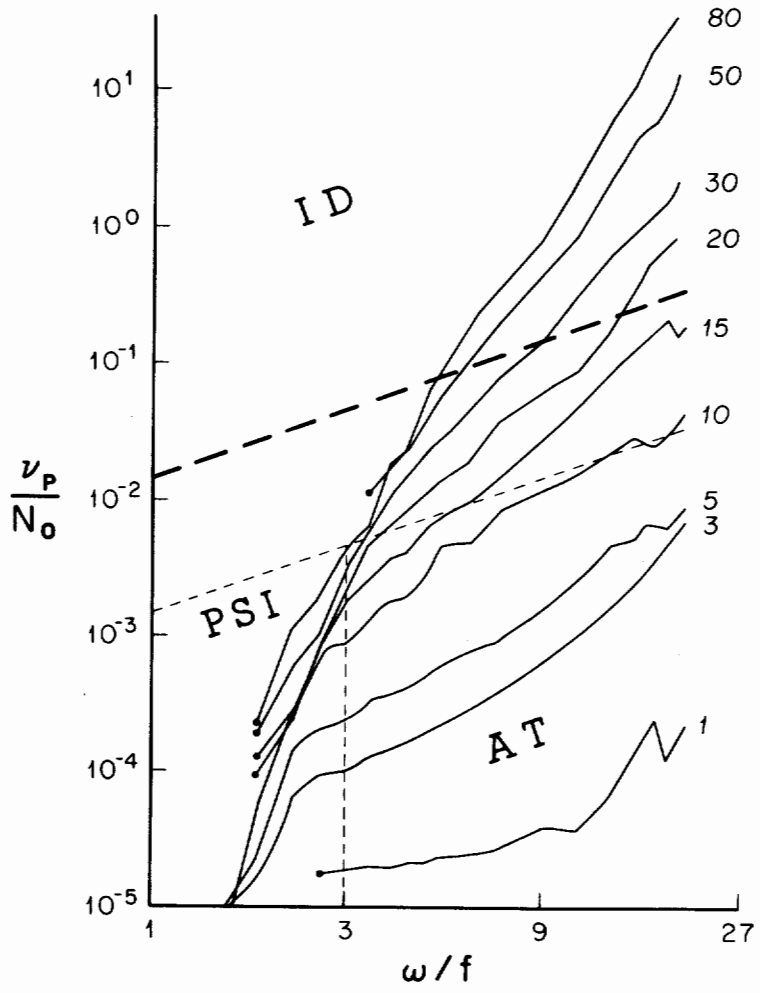

Figure 6. A summary of numerical transport results using the GM76 spectrum. Curves are labelled by value of modenumber.

internal waves in the I.D. domain. Their analysis is based on a linear equation, makes no weak interaction assumption, and contains the weak resonant interaction results as a special case.

The basic equation for this study takes the form

$$D\nabla^2 w + \nabla^2 \Omega^2 \zeta_z = \frac{\partial^2 \underline{u}}{\partial z^2} \cdot \nabla_h w + \frac{\partial}{\partial z} \left[\frac{\partial \underline{u}}{\partial z} \cdot \underline{f} \times \nabla_h \zeta_z \right] ,$$

$$w = D\zeta_z \tag{11}$$

where

$$\nabla_h = \nabla - \hat{z} \frac{\partial}{\partial z} , \quad D = \frac{\partial}{\partial t} + \underline{u} \cdot \nabla_h ,$$

$$\Omega^2 = \left[\nabla^{-2} (f^2 \frac{\partial^2}{\partial z^2} + N^2 \nabla_h^2) \right]^{1/2} .$$

This equation describes small amplitude internal waves in a vertically sheared horizontal flow. $\underline{u}(\underline{r},t)$ describes the flow which results from a superposition of linear near-inertial frequency internal waves. ζ_z is the vertical fluid displacement and w the vertical velocity. Ω is a frequency operator for internal waves. The usual Taylor-Goldstein equation[28] is obtained by setting the Coriolis frequency term equal to zero on the RHS. On the other hand, if both terms on the RHS are ignored the resulting equation is shown by Meiss and Watson to be equivalent to Induced Diffusion. Since the terms on the RHS can be shown to be larger than any other omitted in the derivation from the full Euler equations (notably the nonlinear convective velocity term), these two terms can be regarded as the leading corrections to the I.D. aprroximation and they can be used to estimate its validity (see later).

By Fourier expanding in a basis of linear internal waves (these are solutions of equation (11) when $\underline{u} = 0$), a set of mode equations are obtained which describe the evolution of the small scale amplitudes:

$$\dot{a}_{\underline{k}} + i\omega_{\underline{k}} a_{\underline{k}} = \sum_{\underline{m}} A^{\underline{m}}_{\underline{k}}(t)\, a_{\underline{m}}$$

$$A^{\underline{m}}_{\underline{k}}(t) \equiv h(\underline{k},\underline{m}) \sum_{\underline{\ell}=\text{large scale waves}} (a_{\underline{\ell}}\, \delta_{\underline{k}-\underline{m}-\underline{\ell}} - a^*_{\underline{\ell}}\, \delta_{\underline{k}-\underline{m}+\underline{\ell}}) \tag{12}$$

$$\dot{a}_{\underline{\ell}} + i\omega_{\underline{\ell}} a_{\underline{\ell}} = 0 \quad , \quad \omega_{\underline{\ell}} \approx f \quad .$$

A subscript $\underline{\ell}$ denotes the long waves in the system. Since one member of each I.D. triad is a long wave, the evolution equation for a short wave amplitude is linear in all other short wave amplitudes $a_{\underline{m}} = \underline{k} \pm \underline{\ell}$. The large scale amplitudes execute simple harmonic oscillations at near-inertial frequencies with their statistics described by the GM spectrum. The coefficient $h(\underline{k},\underline{m})$ is an appropriate long wavelength limit of the dynamical coefficients appearing in equation (1).

Mode equation (12) is a linear stochastic differential equation with Gaussian fluctuating coefficients. These are simplifying features which Meiss and Watson exploit in deriving a Langevin equation for the relaxation of small scale amplitudes. This equation has the form

$$\frac{d}{dt}\langle a_{\underline{k}}(t)\rangle = -(i\omega_{\underline{k}} + \gamma(t))\langle a_{\underline{k}}(t)\rangle \quad . \tag{13}$$

The real part of $\gamma(t)$ determines the relaxation rate. It is a time dependent quantity in terms of which an e- folding rate constant ν is defined as

$$\int_0^{\nu^{-1}} \mathrm{Re}\,\gamma(t)\,dt = 1 \tag{14}$$

In the I.D. limit an <u>exact</u> expression for $\gamma(t)$ is obtained:

$$\gamma(t) = \pi \sum_{+,-} \int d\underline{\ell}\, d\underline{m}\; h_I^2(\underline{k},\underline{m})\; D_{\pm}(t)\; \langle |a_{\underline{\ell}}|^2 \rangle\; \delta_{\underline{k}-\underline{m}+\underline{\ell}}$$

where

$$D_{\pm}(t) = \frac{1}{\pi}\int_0^t d\tau\, e^{i(\omega_{\underline{k}} - \omega_{\underline{m}} \pm \omega_{\underline{\ell}})\tau} \quad . \tag{15}$$

and h_I is the appropriate limit of h. All time dependence is contained in the quantity $D_{\pm}$, which in the "static" limit

$$t \gg \frac{1}{\omega_{\underline{k}} - \omega_{\underline{m}} \pm \omega_{\underline{\ell}}}$$

becomes a frequency delta function. The resulting (approximate) expression for the rate constant becomes <u>identical</u> to the resonant weak interaction rate ν_p which gave rise to the troublesome I.D. curves in Figures 5 and 6.

To determine the accuracy of the I.D. rates (15) requires consideration not only of the coefficient h_I, but also the corrections from terms on the RHS of equation (11). Meiss and Watson use perturbation theory to show this correction is never greater than 10% in a domain extending in frequency from 5-31 f and in modenumber from 10-250. The evaluation of the exact expression (15) can be concluded as giving accurate I.D. rates. Figure 7 displays these rates. They are seen to be substantially lower than those predicted by weak interaction theory, being within a factor of ten of the linear frequency even at the highest modenumbers. It is important to note that the linear frequency curve <u>does not</u> this time signify a necessary breakdown of the calculation since the new rates were obtained from a linear equation. These latest results therefore represent a considerable extension of the domain in which plausible

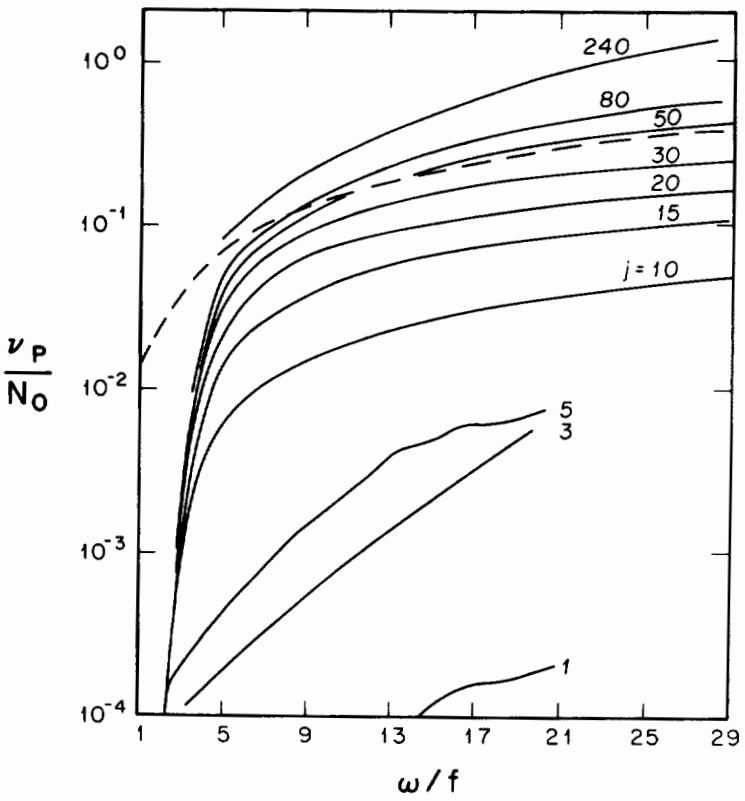

Figure 7. Curves of relaxation rate versus linear frequency obtained by Meiss and Watson using an "exact" descripton of the Induced Diffusion domain. No weak interaction assumption was needed to obtain these curves.

computations of energy transport exist, and if we take these results in conjunction with those of weak interaction theory at low frequencies and modenumbers, the domain is full.

SUMMARY

In this review we have avoided asking whether it is valid to model internal wave interactions using a modal description. This crucial question is discussed elsewhere in these proceedings[29]. A brief survey of modal calculations of energy transfer within the oceanic internal wavefield has been given, and we have indicated that plausible results are obtained by patching together results using weak interaction theory at low frequencies and modenumbers with those based on a modification of the Taylor-Goldstein equation at high frequencies

and modenumbers. These latter results show energy transfer rates substantially lower than those predicted by weak interaction theory, however McComas' appealing "scenario for the genesis and maintenance of the universal (internal wave) spectrum"[24] requires no essential modification. We close by repeating this scenario:

..."Energy input at high frequencies is redistributed by the Induced Diffusion and Elastic Scattering Mechanisms to the universal spectrum of the deep ocean. The main energy input is at small vertical wavenumber (modenumber) and at low frequencies. The low frequency energy is transferred directly to high vertical wavenumber (modenumber) near-inertial waves. This causes an increase in the total shear of the wavefield, which eventually goes unstable. Turbulence is created and internal wave energy is lost. The loss is most important at the small scales because these waves are significantly depleted. The high frequency waves are renewed by a cascade of energy, possibly accompanied by readjustment in spectral shape, in the Induced Diffusion (steady state) region. The low frequency waves are renewed by the Parametric Subharmonic Instability mechanism directly from the main energy source, and the cycle begins again."

REFERENCES

1. C.J.R. Garrett and W. H. Munk, Geophys. Fluid Dyn., 2, 225, (1972); J. Geophys., 80, 291, (1975); Ann. Rev. Fluid Mech., 11, 339, (1979)
2. W. H. Munk, Evolution of Physical Oceanography, edited by B. A. Warren, and C. Wunsch, 264, (1981)
3. K. J. Hasselmann, J. Fluid Mech., 12, 481, (1962); J. Fluid Mech., 15, 273, (1963); J. Fluid Mech., 15, 385, (1963); Rev. Geophys. and Space Phys., 4, 1, (1966); Proc. Roy. Soc., A299, 77, (1967).
4. Identical equations are found in many branches of physics, e.g., plasma, laser, and solid state.
5. P. Ripa, J. Fluid Mech., 103, 87, (1981).
6. F. Henyey, Hamiltonian Description of Internal Wave Dynamics (preprint, 1981).
7. P. Muller, and D. J. Olbers, J. Geophys. Res., 80, 3848, (1975).
8. D. J. Olbers, J. Fluid Mech., 74, 375, (1976).
9. C. H. McComas, and F. P. Bretherton, J. Geophys. Res., 82, 1397, (1977).
10. J. D. Meiss, N. Pomphrey, and K. M. Watson, Proc. Natl. Acad. Sci. (USA), 76, 2109, (1979).
11. An Eulerian derivation is required for these. Ripa (Ref. 5) gives coupling coefficients between Eddy Modes and Internal Waves when N = constant and coriolis force = 0.
12. D. J. Benney, and P. G. Saffman, Proc. Roy. Soc., A289, 301,(1966).
13. R. C. Davidson, J. Plasma Physics, 1, 341, (1967); Methods in Nonlinear Plasma Theory, (Academic Press, New York, 1972).
14. D. J. Benney, and A. C. Newell, Studies in Appl. Math., 48, 29, (1969).
15. J. Meiss (these proceedings) describes a method of trajectory analysis which obtains statistical properties of test wave systems.
16. For other physical systems (dispersion relations) resonance matching occurs first with wave quartets. The surface wave-surface wave interaction is one example.
17. G. M. Zaslavskii, and R. Z. Sagdeev, Soviet Physics JETP, 25, 718, (1967).

18. G. M. Zaslavskii, and B. V. Chirikov, Soviet Physics USPEKI, 14, 549, (1972).
19. N. Pomphrey, J. D. Meiss, and K. M. Watson, J. Geophys. Res., 85, 1085, (1980).
20. This quantity was derived in reference 19 from an application of the fluctuation-dissipation theorem.
21. K. Kenyon, J. Mar. Res., 26, 208, (1968) used equation (5) to compute energy transfer rates in an ocean with linear stratification for a low-mode, pre-GM spectrum.
22. K. D. Leaman, J. Phys. Oceanog., 6, 894, (1976).
23. K. M. Watson, (these proceedings, 1981).
24. C. H. McComas, J. Phys. Oceanog., 7, 836, (1977). This paper contains the "scenario for genesis and maintenance of the universal (internal waves) spectrum" mentioned in the introduction and quoted in the summary.
25. C. H. McComas, and P. Muller, The dynamic balance of internal waves (submitted to J. Phys. Oceanog., 1980).
26. G. Holloway, J. Phys. Oceanog., 10, 906, (1980).
27. J. D. Meiss, and K. M. Watson, Internal wave interactions in the Induced Diffusion approximation (submitted to J. Fluid Mech., 1980).
28. F. P. Bretherton, Quart. J. Roy. Met. Soc., 92, 466, (1966).
29. F. Henyey, (These Proceedings).